3D Numerical Investigation of Face Stability in Tunnels with Unsupported Face

DIMITRIOS GEORGIOU (dgeorgiou@mail.ntua.gr)
National Technical University of Athens: Ethniko Metsobio Polytechneio
ALEXANDROS KALOS
National Technical University of Athens: Ethniko Metsobio Polytechneio
MICHAEL KAVVADAS
National Technical University of Athens: Ethniko Metsobio Polytechneio

Research Article

Keywords: unsupported tunnel faces , 3D numerical analyses, tunnel faces

Posted Date: April 13th, 2021

DOI: https://doi.org/10.21203/rs.3.rs-397369/v1

Version of Record: A version of this preprint was published at Geotechnical and Geological Engineering on June 24th, 2021. See the published version at https://doi.org/10.1007/s10706-021-01900-1.

3D numerical investigation of face stability in tunnels with unsupported face

D. Georgiou[1], A. Kalos[2] and M. Kavvadas[3]

[1] MSc Mining Engineer, National Technical University of Athens, Greece, dgeorgiou@mail.ntua.gr

[2] PhD Civil Engineer, National Technical University of Athens, Greece, alkalos@central.ntua.gr

[3] Professor, National Technical University of Athens, Greece, kavvadas@central.ntua.gr

ABSTRACT

The paper studies the stability of unsupported tunnel faces by analyzing the results of a large number of 3D numerical analyses of tunnel faces, in various ground conditions and overburden depths. The analyses calculate the average face extrusion (U_h) by averaging the axial displacement over the tunnel face. Limiting face stability occurs when the average face extrusion becomes very large and algorithmic convergence becomes problematic. Using the results of the analyses, a dimensionless "face stability parameter" is defined, which depends on a suitable combination of ground strength, overburden depth and tunnel width. The face stability parameter correlates very well with many critical tunnel face parameters, like the safety factor of the tunnel against face instability, the average face extrusion, the radial convergence of the tunnel wall at the excavation face, the volume loss and the deconfinement ratio at the tunnel face. Thus, semi-empirical formulae are proposed for the calculation of these parameters in terms of the face stability parameter. Since the face stability parameter can be easily calculated from basic tunnel and ground parameters, the above critical tunnel parameters can be calculated, and conclusions can be drawn about tunnel face stability, volume loss and the deconfinement ratio at the excavation face which can be useful in preliminary tunnel designs.

1 INTRODUCTION

Control of face stability is very important in tunnelling, as incidents of face instability are frequent, severely affect the cost and construction schedule of tunnels and can damage surface structures and utilities in shallow urban tunnels. In mechanized tunnelling with active face pressure (e.g. EPB and Slurry TBMs), the risk of face instability is controlled by the applied face pressure, which is usually adjusted empirically from past performance in "similar" conditions. In tunnelling with conventional techniques (SCL / NATM), face stability is usually assessed empirically, by subjective comparison of the excavation face with past behaviour of faces under "similar" conditions, occasionally by simplified limit equilibrium analyses (e.g. Leca & Dormieux, 1990; Anagnostou & Kovari, 1996; Kim & Tonon, 2010), and rarely by numerical analysis or systematic measurements of axial face movements (face extrusion). When the risk of face instability is considered unacceptable in SCL / NATM tunnels, the size of the excavation face is reduced or active face support measures are applied, such as fiber-glass (FG) nailing, forepoling, or even leaving a ground wedge on the face. The main reason of the extensive empiricism in assessing face stability, is that quantitative assessment of the risk of face instability requires the definition of a suitable "safety factor", and its calculation using complex three-dimensional (3D) numerical analyses with realistic constitutive models and suitably measured/estimated ground parameters. Although seemingly trivial, even the definition of a "safety factor" for face stability analyses is not always straight forward, let alone its numerical calculation.

In mechanized tunnelling, the safety factor against face instability is usually defined as the ratio of the applied face pressure to the minimum face pressure required for stability. Calculation of the safety

factor requires determination of that minimum face pressure for stability, which is usually achieved by a variance of the increased external load method (Zienkiewicz et al, 1975) via a series of numerical analyses with gradually decreasing face pressure until the tunnel face becomes unstable (i.e., until the numerical algorithm ceases to converge, or face displacements start to increase rapidly). Similar definition of the safety factor and calculation techniques can be used in conventional tunnelling with supported excavation faces, e.g. in cases where the tunnel face is supported by a grid of fiber-glass nails providing an "equivalent" face pressure.

In the very common case of conventional tunnelling with unsupported excavation face, the "safety factor" against face instability can be defined (and calculated) as the ratio of some "strength" over a corresponding "applied shear stress". This definition is straight forward when ground strength is modelled via perfect plasticity with the Mohr-Coulomb (MC) failure criterion, i.e., in:

1. Analytical methods (e.g. Horn 1961, Atkinson & Mair 1981, Panet 1995, Anagnostou & Kovari 1996), which calculate the safety factor of the tunnel face on a suitably selected potential failure surface, by some form of limit equilibrium of a critical ground wedge at the excavation face. These methods usually have limited accuracy and applicability, because of the simplifying assumptions about the selected wedge for a complex 3D problem as the tunnel excavation face.
2. Numerical methods, where the "safety factor" is usually defined and calculated by the Strength Reduction Method (Zienkiewicz et al, 1975), i.e., by performing a series of analyses with gradually reducing ground strength, until the tunnel face becomes unstable (i.e., until the numerical algorithm ceases to converge, or face displacements start to increase rapidly). In such analyses, the safety factor is the inverse of the strength reduction factor causing face instability. Useful design charts are often produced for the safety factor versus ground strength, tunnel depth and size (e.g. Kavvadas et al 2009, Prountzopoulos 2012).

The above methods exploit that, in the MC failure criterion, ground strength is a linear combination of cohesion (c) and friction angle (tanϕ); thus, a single "strength reduction factor" can be applied to both components of strength to cause face instability, with the safety factor being the inverse of that factor.

When ground behaviour is modelled more realistically than Mohr-Coulomb perfect plasticity, investigation of face stability requires the use of numerical analyses. Published literature on numerical analyses of face stability in tunnels with unsupported face using such constitutive laws (e.g. based on the Hoek-Brown failure criterion and/or hardening/softening plasticity) is very sparse, because such analyses are usually problem-specific, i.e., they check if a specific tunnel face is stable, by testing the convergence of the numerical algorithm for given ground and geometrical parameters, but are difficult to generalise in other cases. Furthermore, if the analysis predicts a stable tunnel face (i.e., the algorithm converges with finite face deformations), it is not easy to define the "safety factor" or calculate the available margin from face instability. The reason of this difficulty is that, in constitutive laws other than Mohr-Coulomb perfect plasticity, ground strength is controlled by non-linear combinations of model parameters, rendering inapplicable the strength reduction method. Furthermore, other analogous techniques (like increasing suitable external loads until failure) cannot be applied in tunnel excavation with an unsupported face, because a stable tunnel face does not have any external load (face pressure is zero). This common problem becomes evident in designs attempting to apply the "partial factor method" in Ultimate Limit State (ULS) analyses of stability problems with ground failure controlled by criteria other than Mohr-Coulomb perfect plasticity and/or cases where ground failure is not caused by external loads as in bearing capacity of footings (see e.g. Frank et al, 2004; Franzen et al, 2019).

In conclusion, although numerical analyses can be performed to check if a tunnel face is stable for specific ground and geometrical parameters, there is lack of guidance on assessing the available safety factor of unsupported tunnel faces. Even in cases where complex 3D numerical analyses are performed to study specific tunnel conditions, it is useful to have guidance on the effects of varying ground conditions and/or tunnel depth on face stability, without having to perform additional analyses for

each case or, at least, it is useful to have guidance in optimally selecting the required analyses of face stability, among the usually wide range of ground conditions and tunnel depths in practical tunnelling problems. In such cases, it is useful to have guidance from results of full 3D numerical models, which are more accurate than axi-symmetric tunnel models commonly used in face stability analyses (e.g. Bernaud & Rousset 1996, Graziani et al 2005), especially in shallow tunnels where the effect of gravity is more pronounced and conditions of face instability are more frequent and catastrophic.

The present paper attempts to fill that gap, by providing a semi-empirical expression of an equivalent safety factor of face stability in tunnels with unsupported face, in terms of dimensionless quantities of ground strength, tunnel depth and diameter. The safety factor of face stability is obtained from a dimensionless "face stability parameter" (Λ_f) which is found (numerically) to control the average "face extrusion" (U_h = average axial displacement of the excavation face) for a wide range of ground strengths, failure modes, tunnel depths and sizes. The paper also proposes semi-empirical expressions to calculate the average face extrusion (U_h) and the degree of deconfinement (λ) at the tunnel face, in terms of the controlling face stability parameter (Λ_f). These expressions are derived from the results of a large set of three-dimensional (3D) numerical analyses of the excavation of shallow and deep tunnels with unsupported face in various ground conditions, using the Mohr-Coulomb failure criterion in shallow tunnels and the Hoek-Brown failure criterion in deep tunnels. The analyses focus on the behaviour of the excavation face, by calculating the average face extrusion (U_h), suitably normalized to give a dimensionless "face extrusion parameter" (Ω_f). The results of the analyses show that the face extrusion parameter (Ω_f) is correlated well with the "face stability parameter" (Λ_f) which depends on ground strength, tunnel depth and diameter. It is shown that, as Λ_f decreases and approaches unity, the face extrusion parameter (Ω_f) starts to increase rapidly, indicating incipient face instability. This permits to define the safety factor of an unsupported tunnel face (SF_f) by the face stability parameter (i.e., $SF_f = \Lambda_f$) and thus calculate the safety factor of an unsupported tunnel face and establish the relationship among ground strength, tunnel depth and size corresponding to limiting face instability ($\Lambda_f = 1$). The proposed semi-empirical relationship between Λ_f and Ω_f can be used to calculate the average face extrusion (U_h), the radial wall convergence (U_R) and deconfinement ratio (λ) for various combinations of ground strength, tunnel depth and size. The proposed relationship can be used in preliminary calculations of the safety factor and the degree of deconfinement of the tunnel excavation face, in conventionally excavated tunnels with unsupported face.

2 NUMERICAL ANALYSES

A large set of three-dimensional (3D) numerical analyses were performed, using the Finite Element Code Simulia Abaqus, for the excavation of shallow and deep tunnels with unsupported face and a wide range of ground properties and tunnel depths. Oval-shaped tunnel sections were studied, having width D = 10m and D = 6m (Figure 1).

Shallow tunnels:

In shallow tunnels, the overburden depth (H), measured from the tunnel axis up to the ground surface, varied in the range H = 15 to 30m, with examined cases: H/D = 2.5, 3.5 and 5. Eight-node hexahedral finite elements were used in the analysis (Figure 2). Following a sensitivity analysis, the extent of the finite element mesh was sufficiently large to minimize boundary effects in all directions. The finite element mesh included the left half of the tunnel, because the tunnel section is symmetrical with respect to the vertical axis. The tunnel was excavated in a single phase (full face excavation) with excavation steps of 1m (equal to the size of the elements in the axial direction). In each excavation step, a relatively stiff, 30cm thick, shotcrete liner was installed on the tunnel wall (full ring) 2m behind the excavation face. The shotcrete liner was modelled by 4-noded shell elements, as linearly elastic

with a relatively low concrete E modulus equal to 10 GPa to account for concrete setting time. To eliminate end effects, the conditions at the excavation face were studied when tunnel excavation had advanced to a distance L = 4-6 D from the start boundary, leaving a clear distance 5-7 D from the end boundary (ahead of the tunnel face). Parametric analyses by varying the geometrical and stiffness parameters have shown that the above simplifying assumptions have negligible effects on the results at the excavation face.

The study included relatively stiff ground conditions with unit weight $\gamma = 20$ kN/m^3, horizontal geostatic stress coefficient $K_o = 0.5$ and 1.0 and linearly elastic - perfectly plastic behaviour, with elastic modulus (E) and yielding according to the Mohr-Coulomb criterion (c = cohesion, ϕ = friction angle). Table 1 shows the sets of ground parameters used in the parametric analyses.

Table 1: Sets of ground parameters used in the analyses of shallow tunnels

E (*MPa*)	c (*kPa*)	φ (°)	σ_{cm} (*kPa*)
80	20.0	22.5	59.9
100	20.0	25.0	62.8
120	25.0	25.0	78.5
150	30.0	25.0	94.2
170	30.0	30.0	103.9
200	50.0	30.0	173.2

In all cases, the elastic Poisson ratio was v = 0.33. According to the Mohr-Coulomb failure criterion, the "ground strength" (σ_{cm}), equivalent to the Uniaxial Compressive Strength, was calculated by the formula:

$$\sigma_{cm} = 2c\ tan\left(45° + {}^{\varphi}/_{2}\right) \qquad (1a)$$

The total number of numerical analyses for the shallow tunnels was 72 (two tunnel sizes, three tunnel depths, two K_o values, and six sets of material parameters).

Deep tunnels:

In deep tunnels, the overburden depth was H = 100, 150 and 200m. The Finite Element mesh was similar to that shown in Figure 2, with higher overburden depth. Tunnel excavation and liner construction followed the same procedure as for the shallow tunnels.

The study included weak fractured rock with unit weight $\gamma = 25$ kN/m^3, horizontal geostatic stress coefficient $K_o = 0.5$ and 1.0, intact rock properties $\sigma_{ci} = 10$ MPa and $E_i = 2000$ MPa, Poisson ratio v = 0.33 and Geomechanics Strength Index in the range GSI = 15 to 45. The rockmass was assumed linearly elastic - perfectly plastic, yielding according to the Generalised Hoek-Brown failure criterion (Hoek et al, 2002) with various parameters (m_b, s, a). Table 2 shows the sets of rockmass parameters used in the parametric analyses.

Table 2: Sets of rockmass parameters used in the analyses of deep tunnels

GSI	m_b	s	a	σ_{cm} (*MPa*)	E_m (*MPa*)
15	0.480	7.9×10^{-5}	0.561	0.36	72.9
25	0.687	2.4×10^{-4}	0.531	0.53	119.7
35	0.981	7.3×10^{-4}	0.516	0.79	226.8
45	1.403	2.0×10^{-3}	0.508	1.17	447.3

The "rockmass strength" (σ_{cm}) and "rockmass modulus" (E_m) for the various GSI values were calculated by the following empirical formulae (Litsas et al 2017, Hoek & Diederichs 2006):

$$\sigma_{cm} = 0.02\ \sigma_{ci}\ exp\left(\frac{GSI}{25.5}\right) \quad \text{and} \quad E_m = E_i\left[0.02 + \frac{1}{1+\exp[(60-GSI)/11]}\right] \tag{1b}$$

The total number of numerical analyses for the deep tunnels was 48 (two tunnel sizes, three tunnel depths, two K_o values, and four sets of material parameters).

3 FACE EXTRUSION

Each of the numerical analyses calculates the axial displacement (face extrusion) at all integration points on the tunnel face when tunnel excavation has advanced far from the start and end boundaries. These values are averaged over the tunnel face to give an "average face extrusion" (U_h) which is then normalized by the tunnel width (D) and a modulus-to-depth factor (E / p_o) to give the dimensionless "face extrusion parameter" (Ω_f):

$$\Omega_f = \left(\frac{U_h}{D}\right)\left(\frac{E}{p_o}\right) \tag{2}$$

where E is the elastic Young modulus of the ground (soil or rockmass) and $p_o = 0.5\ (1 + K_o)\ \gamma\ H$ is the average overburden pressure at the tunnel axis (average of vertical and horizontal geostatic stresses).

From the 72+48 = 120 numerical analyses, the present database includes the results of 83 analyses (51 shallow tunnels and 32 deep tunnels), as the remaining 37 (21+16) analyses failed to converge, because the combination of ground strength and tunnel depth (ground stress) produced uncontrollable face extrusions (too low strength for the tunnel depth). Each calculated value of the face extrusion parameter (Ω_f) was then correlated with the corresponding values of various forms of strength-to-stress ratios, with the objective to select the optimal form (giving the best correlation).

Figure 3a plots the calculated face extrusion parameter (Ω_f) versus the corresponding value of the classical ratio of rockmass strength (σ_{cm}) to average overburden pressure (p_o), often used to describe tunnel behaviour (e.g. Hoek, 2000). The correlation of the two parameters is poor, especially at low strength-to-stress values ($\sigma_{cm} / p_o < 0.5$), where face stability problems are expected, indicating that σ_{cm} / p_o is not a proper parameter for face stability analyses.

Figure 3b plots the calculated face extrusion parameter (Ω_f) with the selected (optimal) strength-to-stress ratio, the "face stability parameter" (Λ_f), a semi-empirical dimensionless parameter combining ground strength σ_{cm} and overburden stress, expressed via the tunnel depth (H), K_o parameter, and tunnel size (D) by the formula:

$$\Lambda_f = 3.8\left(\frac{\sigma_{cm}}{\gamma H\sqrt{1+(2/3)K_o}}\right)\left(\frac{H}{D}\right)^{0.35} \tag{3}$$

The best fit curve of the data points shown in Figure 3b is expressed by the formula:

$$\Omega_h = 1.4\ \Lambda_f{}^{-1.2} \tag{4}$$

This formula can estimate the face extrusion parameter (Ω_f) and, via equation 2, calculate the average face extrusion (U_h) for given Λ_f, i.e., a tunnel with of size (D), overburden depth (H) in ground with strength (σ_{cm}). Control analyses have shown that the above formula can also be used in tunnel shapes different than those shown in the present study (Figure 1), including excavation of the top heading of

a tunnel, via an equivalent tunnel size: D = 1.15 sqrt(A), where A is the section area of the tunnel or phase.

In Figure 3b, large (Λ_f) values correspond to good face stability conditions, i.e., large ground strength, and/or shallow and small size tunnels, with degrading face stability conditions (i.e., increasing face extrusion) as (Λ_f) decreases. The scaling factor "3.8" in the definition of (Λ_f) (equation 3) was selected such that, when $\Lambda_f = 1$, the rate of the face extrusion parameter (Ω_f) increases rapidly, indicating that the tunnel face approaches limiting face stability, although the numerical algorithm converged in about 50% of the models with $\Lambda_f < 1$ giving large face extrusions. Based on this remark, the condition $\Lambda_f = 1$ provides limiting face stability, while tunnel faces with $\Lambda_f < 1$ are considered unstable. At limiting face stability, equations (2), (3) and (4) give the limiting face extrusion and limiting ground strength:

$$\left(\Omega_f\right)_{\lim} = 1.4 \quad \Rightarrow \quad \left(\frac{U_h}{D}\right)_{\lim} = 1.4\left(\frac{p_o}{E}\right) \tag{5a}$$

$$(\sigma_{cm})_{lim} = 0.263\,\gamma H\sqrt{1+(2/3)K_o}\left(\frac{D}{H}\right)^{0.35} \tag{5b}$$

where: $(\sigma_{cm})_{lim}$ is the lowest ground strength to ensure limiting face stability for a given tunnel size (D) and overburden depth (H). For a specific ground type at the excavation face, the available ground strength can be calculated from equation (1a) for soils and equation (1b) for rockmasses and compared to the limiting value (equation 5b) to assess whether the tunnel face is stable or not.

Figure 4 plots the limiting ground strength $(\sigma_{cm})_{lim}$ versus (H/D) for two values of the horizontal geostatic stress coefficient K_o = 0.5 and 1.0. For example, in a tunnel with overburden depth H = 4 D, the limiting ground strength for face stability is: $(\sigma_{cm})_{lim} \approx 0.2\ \gamma\ H$. For a tunnel in soil with friction angle $\phi = 30^o$, the corresponding limiting cohesion is (from equation 1a): $(c)_{lim} \approx 0.058\ \gamma\ H$. For example, for D = 10m, H=40m, γ = 20 kN/m^3 and $\phi = 30^o$, the limiting cohesion for face stability is c = 46 kPa. Lower cohesion values correspond to unstable tunnel face.

The above definition of the face stability parameter (Λ_f) can assist in the calculation of the safety factor (SF_f) of tunnel faces against instability, by defining the safety factor as the ratio of the available ground strength to the corresponding limiting ground strength, and using equations (5b) and (3):

$$SF_f = \frac{\sigma_{cm}}{(\sigma_{cm})_{lim}} = \frac{\sigma_{cm}}{0.263\gamma H\sqrt{1+(2/3)K_o}\left(\frac{D}{H}\right)^{0.35}} = 3.8\left(\frac{\sigma_{cm}}{0.263\gamma H\sqrt{1+(2/3)K_o}}\right)\left(\frac{H}{D}\right)^{0.35} = \Lambda_f$$

Thus, the safety factor of the tunnel against face instability (SF_f) is equal to the face stability parameter (Λ_f), i.e.:

$$SF_f = \Lambda_f = 3.8\left(\frac{\sigma_{cm}}{\gamma H\sqrt{1+(2/3)K_o}}\right)\left(\frac{H}{D}\right)^{0.35} \tag{6}$$

Figure 5 plots the safety factor of the tunnel against face instability (SF) versus the strength-to-stress ratio (σ_{cm} / p_o) for several values of the ratio (H/D) and K_o = 0.50.

Combining equations (2) and (4), the average face extrusion (U_h) for given safety factor (SF_f) is given by the formula:

$$\frac{U_h}{D} = 1.4\left(\frac{p_o}{E}\right)\left(\Lambda_f\right)^{-1.2} \quad \Rightarrow \quad \frac{U_h}{D} = 1.4\left(\frac{p_o}{E}\right)\left(SF_f\right)^{-1.2} \tag{7}$$

Figure 6 plots the predicted average face extrusion (U_h) versus the safety factor of the tunnel face, for typical values of the modulus-to-strength ratio for weak and fractured rockmasses E/p_o = 75, 100 and 150. For $SF_f < 1$, the average face extrusion increases rapidly. At limiting face stability (SF=1), the average face extrusion is equal to 1-2% of the tunnel size (D).

4 RADIAL WALL CONVERGENCE, VOLUME LOSS AND DECONFINEMENT

Figure 7 shows the profile, along the tunnel axis, of the radial convergence (U_R) of the tunnel wall and the distribution of the face extrusion (U_h) on the tunnel face. Radial wall convergence occurs and in the tunnel core, ahead of the tunnel face.

The volume loss (VL) is defined as the reduction (ΔV) of the volume (V) of the core ahead of the tunnel face per unit volume of the core. Volume loss is caused by the radial convergence of the tunnel wall in the core which "squeezes" the core giving face extrusion. Assuming that the profile of the radial wall convergence in the core (length L, tunnel section area A) is approximately linear, with maximum value of the radial wall convergence at the excavation face equal to (U_R), then:

$$\Delta V = \left(\frac{1}{2} U_R\, L\right)(\pi D) \qquad\qquad V = A\, L \tag{8}$$

and the volume loss (VL) is:

$$(VL) = \frac{\Delta V}{V} = \left(\frac{\pi}{2}\right)\frac{\left(U_R/D\right)}{\left(A/D^2\right)} \tag{9}$$

The radial convergence (U_R) of the tunnel wall at the excavation face can be obtained from the average face extrusion (U_h) (calculated via equations 7 and 6) by assuming that the deformation of the core occurs with practically no volume change, i.e., the reduction (ΔV) of the volume of the core is equal to the ground volume extruded at the tunnel face, i.e., $\Delta V = (A\, U_h)$. Combining this equation with equation (8) gives:

$$U_R = \left(\frac{2}{\pi}\right)\frac{\left(A/D^2\right)}{\left(L/D\right)} U_h \tag{10}$$

The examined tunnels have section area $A = 0.75\, D^2$. The length (L) of the core was calculated by correlating the average radial displacement (U_R) at the tunnel face computed in the numerical analyses with the radial displacement predicted from the face extrusion (U_h) via equation (10). The best fit is achieved for L = 0.38 D (Figure 8).

Thus, equation (10) gives (using equation 7):

$$U_R = 1.25\; U_h \quad \Rightarrow \quad \frac{U_R}{D} = 1.75\left(\frac{p_o}{E}\right)\left(\Lambda_f\right)^{-1.2} \tag{11}$$

and the volume loss (VL) can be expressed as (combining equation 9 with 11 and $A = 0.75\, D^2$):

$$VL = 1.83\left(\frac{p_o}{E}\right)\left(\Lambda_f\right)^{-1.2} \tag{12}$$

Figure 9 plots the calculated radial wall convergence (U_R) at the tunnel face (from equation 11) versus the face stability parameter (Λ_f), for typical values of the modulus-to-strength ratio for weak and fractured rockmasses E/p_o = 75, 100 and 150. For typical stable faces (Λ_f = 1 – 2.5), the calculated radial wall convergence (U_R / D) is in the range 0.5 – 2.5%.

Figure 10 plots the calculated volume loss at the tunnel face (from equation 12) versus the face stability parameter (Λ_f), for typical values of the modulus-to-strength ratio for weak and fractured rockmasses E/p_o = 75, 100 and 150. For typical stable faces (Λ_f = 1 – 2.5), the calculated volume loss is in the range 0.5 – 2.5%.

In 2D (plane strain) numerical analyses of tunnel excavation and support, the deconfinement ratio (λ) is used to calculate a fictitious radial internal pressure (p_i) which produces the same inward radial convergence (U_R) of the tunnel wall as a corresponding 3D model which, unlike the 2D model, includes the effects of the excavation face (Figure 7). By definition, the internal pressure (p_i) is related to the deconfinement ratio (λ) by the formula:

$$p_i = \left(1-\lambda\right) p_o \tag{13}$$

The relationship between (U_R) and (p_i) (or λ) is the convergence–confinement relationship, calculated using several methods, such as Duncan Fama (1993), Panet (1995), Kavvadas (1998), Carranza–Torres et al (2002) and Carranza–Torres (2004).

The deconfinement ratio (λ) and the corresponding internal pressure (p_i) vary with the distance (x) from the excavation face. As the radial wall convergence increases along the tunnel axis, and the corresponding internal pressure decreases, the deconfinement ratio varies from λ = 0 far ahead of the excavation face (where wall convergence is zero) to λ = 1 far behind the excavation face (where wall convergence is stabilized to the maximum value). Several semi-empirical formulae have been proposed for the calculation of (λ) at various distances (x) from the excavation face. These formulae are produced by equating the radial convergence (U_R) of the tunnel wall from 2D analyses (applying an internal pressure p_i) with the corresponding radial convergence profile along the tunnel axis from 3D finite element analyses (e.g., Panet 1995, Chern et al. 1998, Vlachopoulos & Diederichs 2009).

The methodology developed above can provide an empirical relationship between the deconfinement ratio (λ) at the tunnel face and the corresponding face stability parameter (Λ_f), by correlating the value of (λ) at the tunnel face, computed using the above convergence–confinement relationships, with the face stability parameter (Λ_f), for each of the 87 numerical analyses studied. Figure 9 plots the results of this correlation using four alternative convergence-confinement methods. The best fit curve of the correlation is:

$$\lambda = 0.25 + 0.75\exp\left(-\Lambda_f / 2\right) \tag{14}$$

Stable tunnel faces (Λ_f > 1) have deconfinement ratios λ = 0.30 - 0.70, with higher λ values for unstable tunnel faces (Λ_f < 1).

5 CONCLUSIONS

The paper studies the stability of unsupported tunnel faces by analyzing the results of a large set (87 Nos) of 3D numerical analyses of tunnel faces, in various ground conditions and overburden depths. The analyses calculate the average face extrusion (U_h) by averaging the axial displacement over the

tunnel face. Limiting face stability occurs when the average face extrusion becomes very large and algorithmic convergence becomes problematic. Using the results of the analyses, a dimensionless "face stability parameter" (Λ_f) is defined (equation 3) which depends on a suitable combination of ground strength (σ_{cm}), overburden depth (H) and tunnel width (D). The (Λ_f) parameter correlates very well with many critical tunnel face parameters, like the safety factor of the tunnel against face instability (equation 6, Figure 5), the average face extrusion (equation 7, Figure 6), the radial convergence of the tunnel wall at the excavation face (equation 11, Figure 9), the volume loss (equation 12, Figure 10) and the deconfinement ratio at the tunnel face (equation 14, Figure 11). Thus, semi-empirical formulae are proposed for the calculation of these parameters in terms of the face stability parameter. Since the face stability parameter can be easily calculated from basic tunnel and ground parameters, the above critical tunnel parameters can be calculated, and conclusions can be drawn about tunnel face stability, volume loss and the deconfinement ratio at the excavation face which can be useful in preliminary tunnel designs. Furthermore, the calculated volume loss can be used to estimate ground surface settlements in shallow tunnels, while the deconfinement ratio can be used in 2D numerical analyses of tunnel excavation and support.

6 ACKNOWLEDGEMENTS

The present PhD thesis research of Mr. D. Georgiou was supported by scholarship funding from the Onassis Foundation and the Evgenides Foundation.

7 NOTATION

A = tunnel section area (m^2)

c = soil cohesion (Mohr-Coulomb failure criterion)

D = tunnel width (m)

E = Young modulus of the ground

E_i = intact rock Young modulus

E_m = rockmass Young modulus

GSI = Geomechanics Strength Index

H = overburden depth measured from the tunnel axis up to the ground surface

L = length of the tunnel core

m_b, s, a = parameters of the Hoek-Brown failure criterion

p_i = fictitious radial internal pressure

p_o = average overburden pressure at the tunnel axis (average of vertical and horizontal geostatic stresses).

SF = safety factor of the tunnel face against instability

U_h = average face extrusion

U_R = radial convergence of the tunnel wall

V = volume of the core, ahead of the tunnel face

VL = volume loss = $\Delta V / V$

K_o = horizontal geostatic stress coefficient

ΔV = reduction of V, due to tunnel wall convergence

Λ_f = face stability parameter

λ = deconfinement ratio

v = Poisson ratio of the ground

σ_{ci} = intact rock strength

σ_{cm} = ground strength (for soils and rockmasses)

ϕ = soil friction angle (Mohr-Coulomb failure criterion)

Ω_f = face extrusion parameter

8 REFRERENCES

Anagnostou G. & Kovári K. (1996) "Face stability conditions with earth-pressure-balanced shields." *Tunnelling and underground space technology* Vol 11 (2), pp 165-173.

Atkinson, J. H., & Mair R. J. (1981) "Soil mechanics aspects of soft ground tunnelling." *Ground Engineering*, Vol 14 (5).

Bernaud D. & Rousset G. (1996) "The new implicit method for tunnel analysis" , *Int J Numer Anal Methods Geomech*, Vol 20, pp 673–690.

Carranza-Torres, C., et al. (2002) "Elasto-plastic analysis of deep tunnels in brittle rock using a scaled form of the Mohr-Coulomb failure criterion." *Proc. of the 5th North American Rock Mechanics Symposium and the 17th Tunnelling Association of Canada Conference*, NARMS-TAC, Toronto, Canada, ed. Hammah et al.

Carranza-Torres, C. (2004) "Elasto-plastic solution of tunnel problems using the generalized form of the Hoek-Brown failure criterion." International Journal of Rock Mechanics and Mining Sciences 41.SUPPL. 1 : 1-11.

Chern JC, Shiao FY, Yu CW (1998) "An empirical safety criterion for tunnel construction". *Proc. of the Regional Symposium on Sedimentary Rock Engineering*, Taipei, Taiwan, pp 222–227.

Duncan Fama ME. (1993) "Numerical modelling of yield zones in weak rocks". *Compr Rock Eng Princ Pract Proj* 1993; 2: 49-75

Frank RC, C Bauduin, R Driscoll, M Kavvadas, N Krebs Ovesen, T Orr, B Schuppener (2004) "*Designers' Guide to EN 1997-1, Eurocode 7: Geotechnical design Part 1: General rules*", Thomas Telford.

Franzén G., M. Arroyo Alvarez de Toledo, A. Lees, M. Kavvadas, A. Van Seters, H Walter, AJ Bond (2019) "Tomorrow's geotechnical toolbox: EN 1997-1: 202x General rules", Proc. of the XVII ECSMGE, Edinburgh, UK.

Graziani A, Boldini D. & Ribacchi R (2005) "Practical estimate of deformations and stress relief factors for deep tunnels supported by shotcrete". *Rock Mech and Rock Eng* 38:345–372.

Hoek, E (2001) "Big Tunnels in Bad Rock". Terzaghi Lecture. *ASCE Journal of Geotechnical and Geoenvironmental Engineering*, Vol. 127, No. 9, pp 726-740.

Hoek E, Carranza-Torres C, Corkum B. (2002) "Hoek-Brown criterion, 2002 edition". In Mining and tunnelling innovation and opportunity, Proc. of the 5th North American Rock Mechanics Symposium

and 17th Conference of the Tunnelling Association of Canada, Hammah R, Bawden W, Curran J, Telesnicki M, editors, Toronto, Canada, pp. 267-73.

Hoek, E. & Diederichs, M.S. (2006). Empirical estimation of rock mass modulus. International Journal of Rock Mechanics and Mining Sciences, 43, 203–215

Leca E. & Dormieux L. (1990) "Upper and lower bound solutions for the face stability of shallow circular tunnels in frictional material," Geotechnique, vol. 40, no. 4, pp. 581–606.

Kavvadas, M. (1998) "Design of Underground Structures". University Notes (in Greek). Graduate Course on Design and Construction of Underground Works. National Technical University of Athens.

Kavvadas, M., G. Prountzopoulos, & K. Tzivakos (2009) "Prediction of face stability in unsupported tunnels using 3d finite element analyses." *Proc. 2nd International Conference on Computational Methods in Tunnelling EUROTUN*. 2009.

Kim S. H. & Tonon F. (2010) "Face stability and required support pressure for TBM driven tunnels with ideal face membrane - Drained case," Tunnelling and Underground Space Technology, vol. 25, no. 5, pp. 526–542.

Litsas D., Sitarenios P. & Kavvadas M. (2017) "Effect of face support pressure on tunnelling induced ground movement", Proc. World Tunnel Congress (WTC 2017), Bergen, Norway.

Lunardi, P. (2008). Design and construction of tunnels: Analysis of Controlled Deformations in Rock and Soils (ADECO-RS). Springer Science & Business Media.

Marinos P. & Hoek E. (2000) "GSI: A geologically friendly tool for rock mass strength estimation" *ISRM international symposium*. International Society for Rock Mechanics and Rock Engineering.

Panet M (1995) Calcul des tunnels par la methode de convergence-confinement. Presses de l'Ecole Nationale des Ponts et Chaussees, Paris

Peck, R. B. (1969) "Deep excavations and tunneling in soft ground." *Proc. 7th ICSMFE*, pp 225-290.

Prountzopoulos, G. (2012) "Investigation of the excavation face stability in shallow tunnels." PhD Thesis, National Technical University, Geotechnical Division, Athens (in Greek).

Vlachopoulos, N. & Diederichs M.S. (2009) "Improved longitudinal displacement profiles for convergence confinement analysis of deep tunnels" Rock Mechanics and Rock Engineering, Vol 42 (2), pp 131-146.

Zienkiewicz O.C, Humpheson C & Lewis R. W. (1975) "Associated and non-associated visco-plasticity in soil mechanics", *Geotechnique*, Vol 25 (4), pp 671–689

Figure 1: Cross sections of the two oval shaped tunnels studied: width D = 10m and 6m and section area A = 75 m^2 and 27 m^2 respectively (A/D^2 = 0.75).

Figure 2: Typical Finite element mesh used in the analyses of the shallow tunnels. The case shown corresponds to tunnel width D = 10m and overburden depth H = 3D = 30m. The different colours of elements close to the surface correspond to element groups that were de-activated for cases with smaller overburden depth.

Figure 3a: Correlation of the face extrusion parameter (Ω_f) with the classical ground strength to overburden pressure ratio (σ_{cm} / p_o) for the results of 83 numerical analyses. The correlation of the two parameters is poor, especially at low strength-to-stress values ($\sigma_{cm} / p_o < 0.5$), where face stability problems are expected.

Figure 3b: Correlation of the face extrusion parameter (Ω_f) with the semi-empirical face stability parameter (Λ_f), defined by equation 3, which achieves optimal correlation for the results of 83 numerical analyses. The figure also shows the best fit curve (equation 4).

Figure 4: Minimum ground strength (σ_{cm}) for limiting face stability versus (H/D)

Figure 5: Safety factor (SF) of the tunnel against face instability (SF) versus the strength-to-stress ratio (σ_{cm} / p_o) for several values of the ratio (H/D) and K_o = 0.50

Figure 6: Average face extrusion (U_h) versus the safety factor (SF) of the tunnel face

Figure 7: Profile of the radial convergence (U_R) of the tunnel wall along the tunnel axis and distribution of the face extrusion (U_h) on the tunnel face (shown in dark green colour). Radial wall convergence occurs and in the tunnel core (shown in brown colour) ahead of the tunnel face (figure adapted from Lunardi, 2008)

Figure 8: Comparison of the average radial displacement (U_R) at the tunnel face computed in the numerical analyses with the radial displacement predicted from the calculated face extrusion (U_h) via equation (10). The best fit is achieved for L / D = 0.76.

Figure 9: Calculated radial wall convergence (U_R) at the tunnel face versus the face stability parameter (Λ_f)

Figure 10: Calculated volume loss at the tunnel face versus the face stability parameter (Λ_f)

Figure 11: Correlation of the deconfinement ratio (λ) at the tunnel face (computed using four convergence–confinement methods) with the face stability parameter (Λ_f) for each of the 87 numerical analyses studied. The figure also shows the best-fit curve (equation 14).

Figures

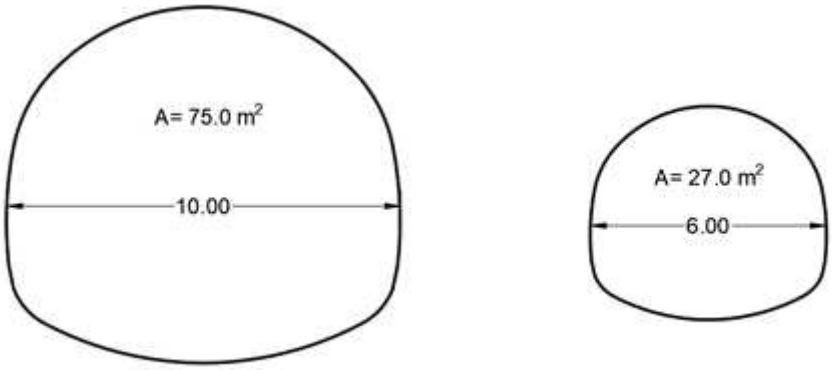

Figure 1

Cross sections of the two oval shaped tunnels studied: width D = 10m and 6m and section area A = 75 m2 and 27 m2 respectively (A/D2 = 0.75).

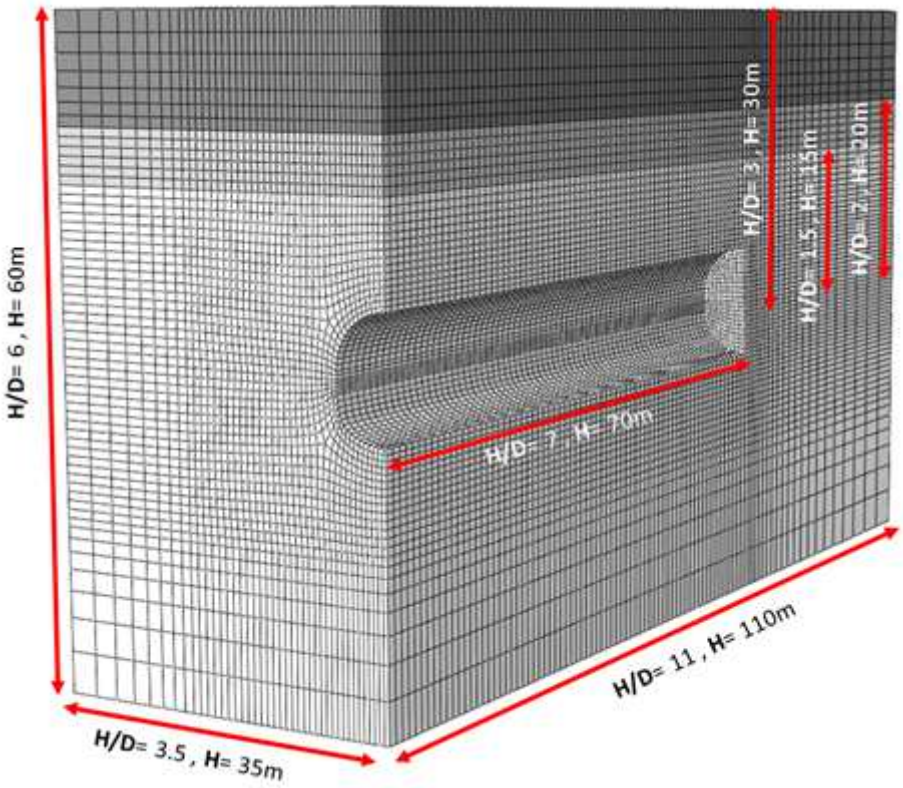

Figure 2

Typical Finite element mesh used in the analyses of the shallow tunnels. The case shown corresponds to tunnel width D = 10m and overburden depth H = 3D = 30m. The different colours of elements close to the surface correspond to element groups that were de-activated for cases with smaller overburden depth.

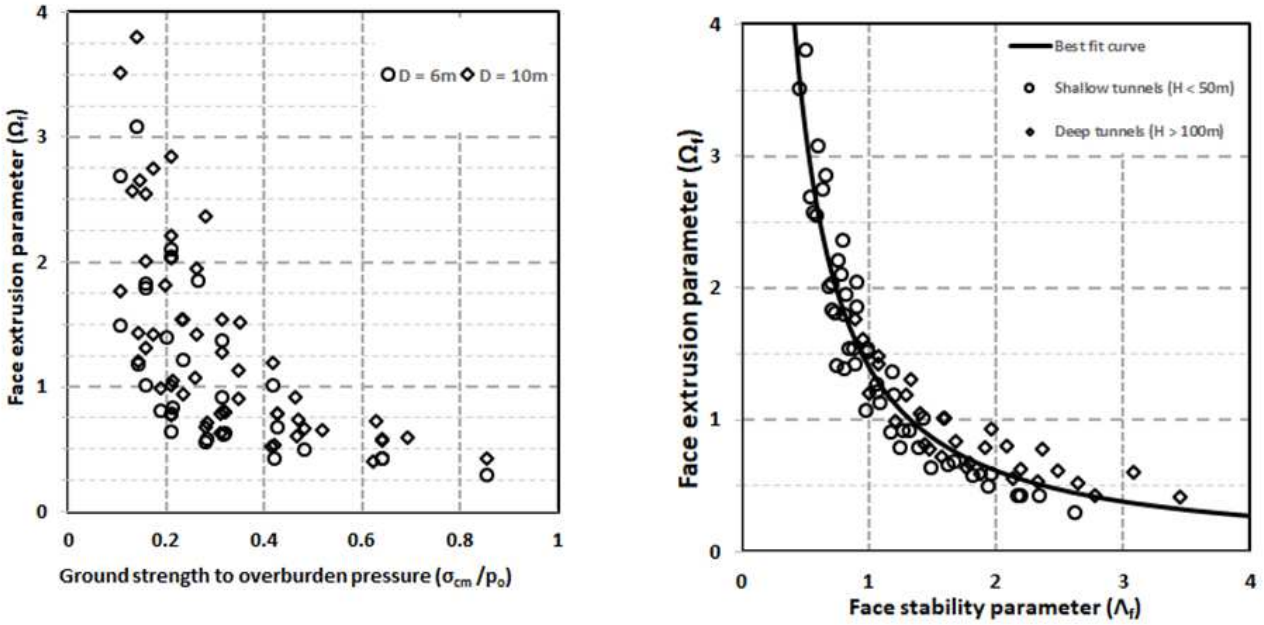

Figure 3

3a: Correlation of the face extrusion parameter (Ωf) with the classical ground strength to overburden pressure ratio (σcm / po) for the results of 83 numerical analyses. The correlation of the two parameters is poor, especially at low strength-to-stress values (σcm / po < 0.5), where face stability problems are expected. 3b: Correlation of the face extrusion parameter (Ωf) with the semi-empirical face stability parameter (Λf), defined by equation 3, which achieves optimal correlation for the results of 83 numerical analyses. The figure also shows the best fit curve (equation 4).

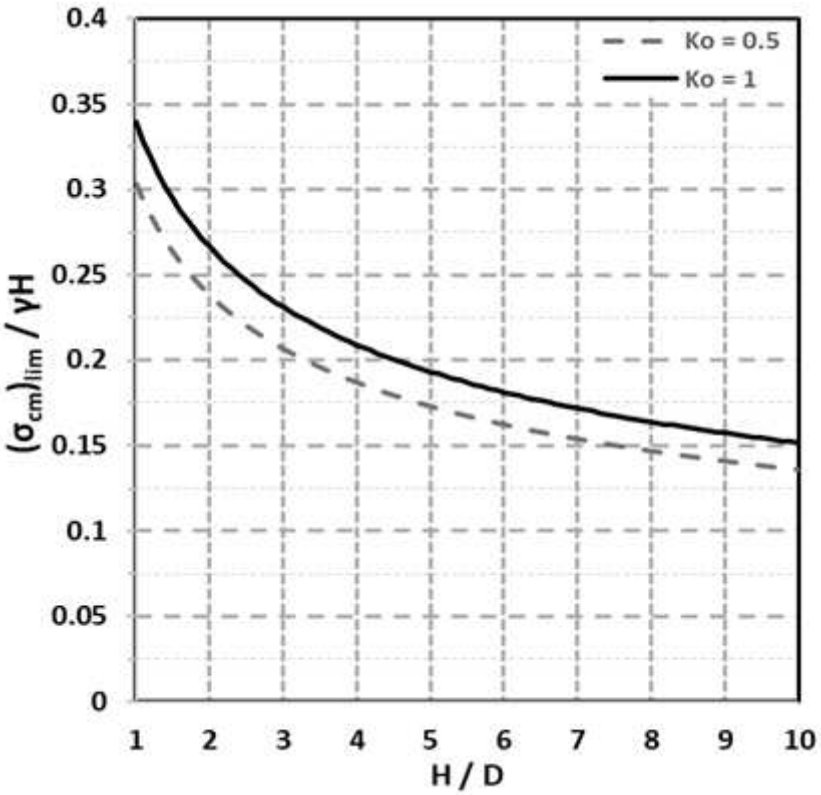

Figure 4

Minimum ground strength (σcm) for limiting face stability versus (H/D)

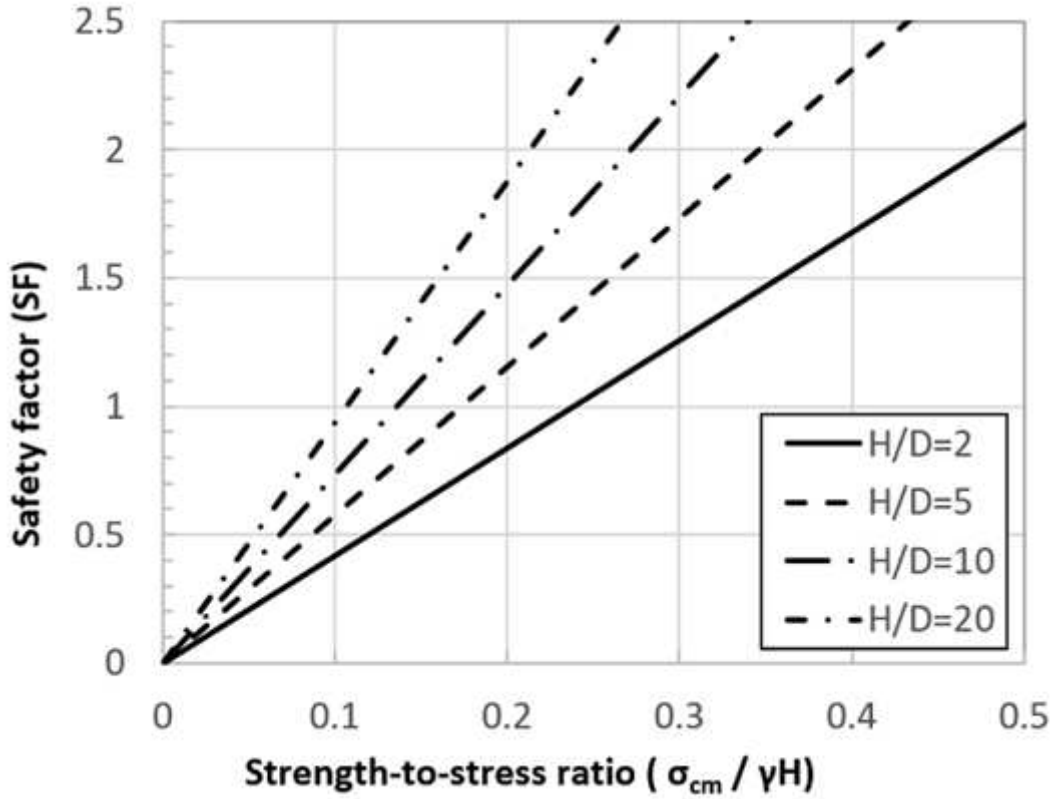

Figure 5

Safety factor (SF) of the tunnel against face instability (SF) versus the strength-to-stress ratio (σcm / po) for several values of the ratio (H/D) and Ko = 0.50

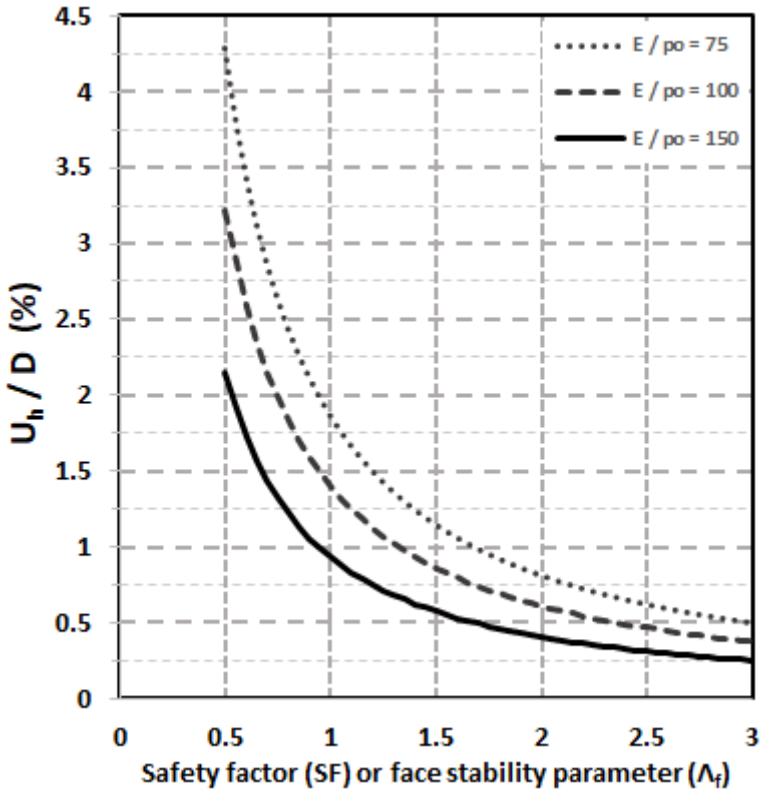

Figure 6

Average face extrusion (Uh) versus the safety factor (SF) of the tunnel face

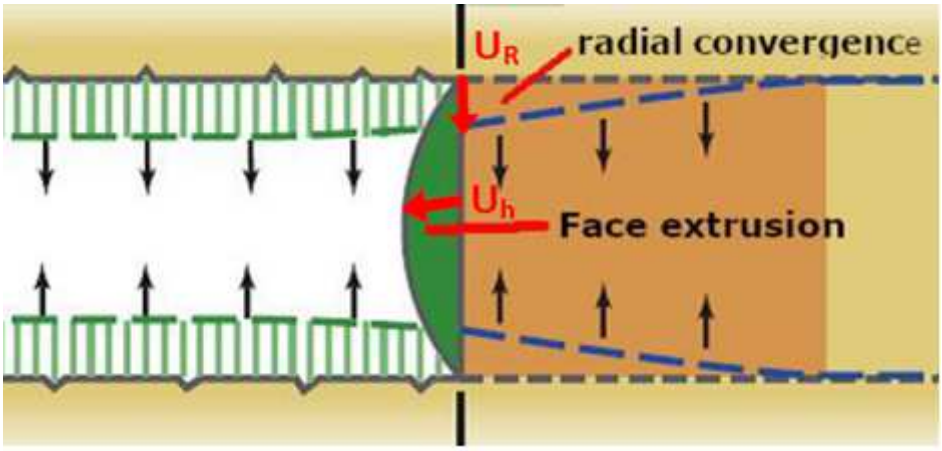

Figure 7

Profile of the radial convergence (UR) of the tunnel wall along the tunnel axis and distribution of the face extrusion (Uh) on the tunnel face (shown in dark green colour). Radial wall convergence occurs and in the tunnel core (shown in brown colour) ahead of the tunnel face (figure adapted from Lunardi, 2008)

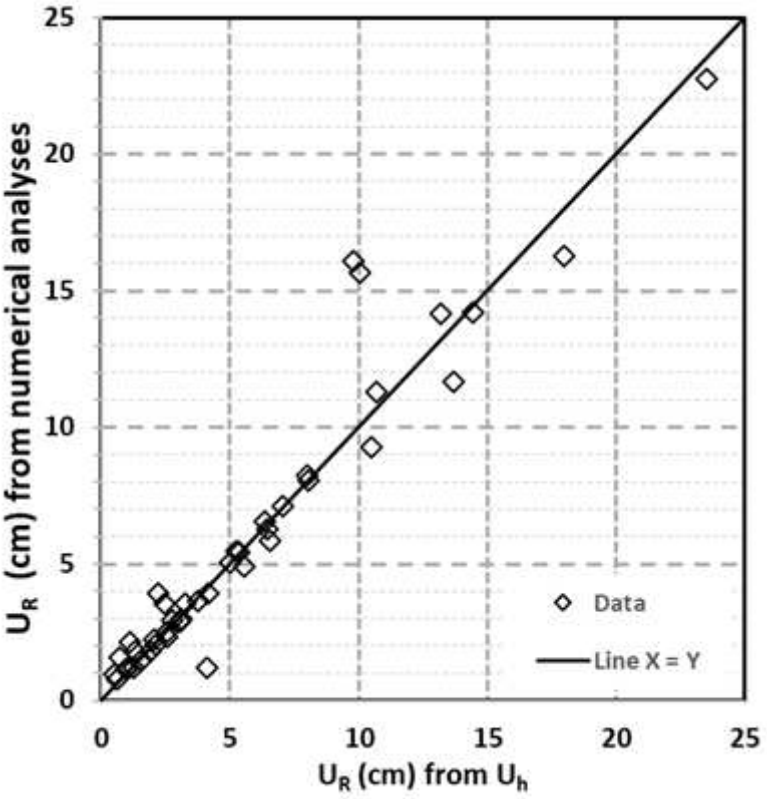

Figure 8

Comparison of the average radial displacement (UR) at the tunnel face computed in the numerical analyses with the radial displacement predicted from the calculated face extrusion (Uh) via equation (10). The best fit is achieved for L / D = 0.76.

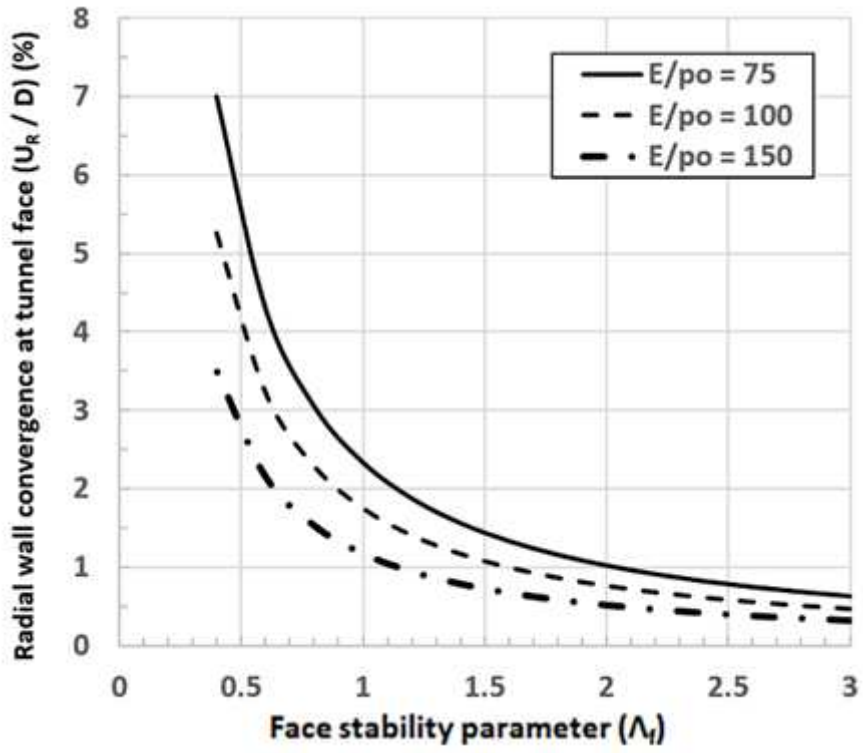

Figure 9

Calculated radial wall convergence (UR) at the tunnel face versus the face stability parameter (Λf)

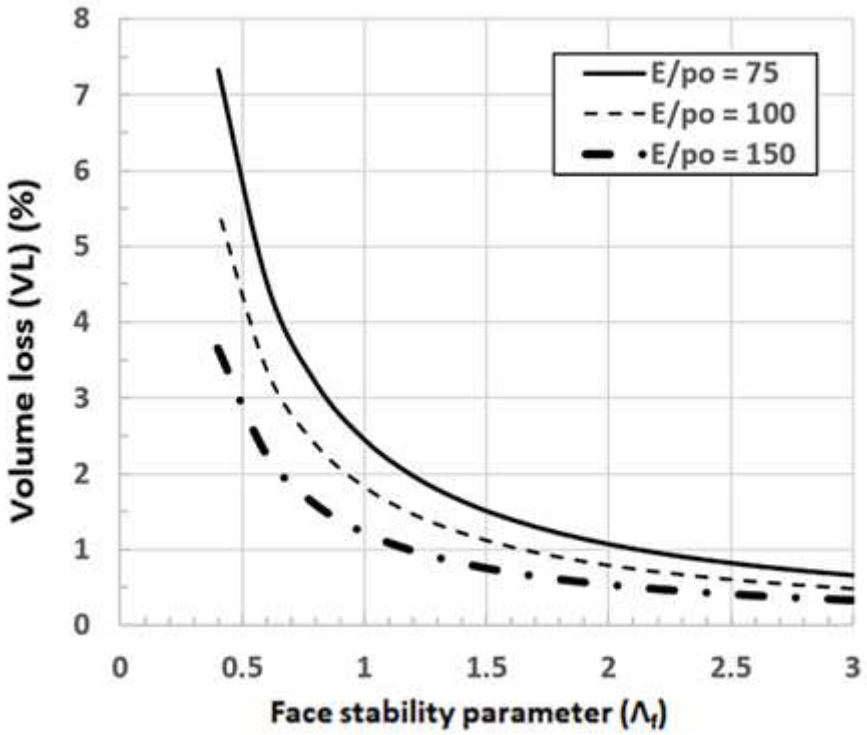

Figure 10

Calculated volume loss at the tunnel face versus the face stability parameter (Λf)

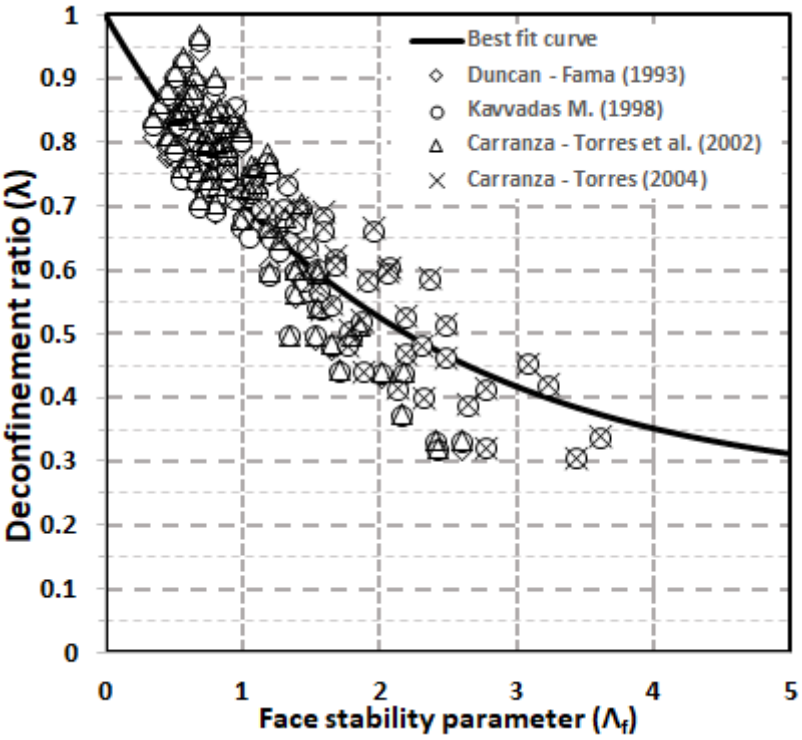

Figure 11

Correlation of the deconfinement ratio (λ) at the tunnel face (computed using four convergence–confinement methods) with the face stability parameter (Λf) for each of the 87 numerical analyses studied. The figure also shows the best-fit curve (equation 14).